

# Soft Matter

Accepted Manuscript



This is an *Accepted Manuscript*, which has been through the Royal Society of Chemistry peer review process and has been accepted for publication.

*Accepted Manuscripts* are published online shortly after acceptance, before technical editing, formatting and proof reading. Using this free service, authors can make their results available to the community, in citable form, before we publish the edited article. We will replace this *Accepted Manuscript* with the edited and formatted *Advance Article* as soon as it is available.

You can find more information about *Accepted Manuscripts* in the [Information for Authors](#).

Please note that technical editing may introduce minor changes to the text and/or graphics, which may alter content. The journal's standard [Terms & Conditions](#) and the [Ethical guidelines](#) still apply. In no event shall the Royal Society of Chemistry be held responsible for any errors or omissions in this *Accepted Manuscript* or any consequences arising from the use of any information it contains.



## Soft Matter

## REVIEW

## Directed Self-Assembly of Gold Nanoparticles to Plasmonic Chains

Chunxiao Xi,<sup>†,a</sup> Paula Facal Marina,<sup>†,b</sup> Haibing Xia,<sup>a,\*</sup> and Dayang Wang<sup>b,\*</sup>Received 00th January 20xx,  
Accepted 00th January 20xx

DOI: 10.1039/x0xx00000x

www.rsc.org/

The plasmonic behavior of metals at the nanoscale is not only appealing for fundamental studies, but also very useful for the development of innovative photonic devices. The past decades have witnessed great progress in colloidal synthesis of monodisperse metal nanoparticles with defined shapes. This has significantly fueled up the research of directing the metal nanoparticles to self-assemble into tailored extended structures, especially low dimensional ones, for a better control and manipulation of the interactions of the metal nanoparticles with light. In parallel, theories for the better description of nanoplasmonics have been increasingly developed and improved. Thus, the present review is focused on the overview of current experimental and theoretical developments in the directed self-assembly of metal nanoparticles with tailored plasmonic properties, which, hopefully, will provide a useful guideline for future researches and applications of nanoplasmonics.

## 1. Introduction

When light interacts with a metal nanoparticle (NP), the electric field of the incoming radiation induces the formation of a dipole on the free electron cloud on the boundary of the nanoparticle, resulting in the collective oscillation of the metal-free electrons with respect to the nanoparticle lattice. The unique resonance frequency which matches this electron oscillation, known as surface plasmon resonance (SPR),<sup>1</sup> strongly depends on the NP size and shape,<sup>2-5</sup> the composition of the NPs,<sup>3</sup> and the nature of the dielectric materials surrounding the NPs.<sup>2, 6-8</sup> In most cases, the SPRs of metal NPs can be easily discerned by the naked eye because the NPs strongly absorb, reflect, and scatter light in the visible frequency spectrum. Further, metal NPs can also transmit light with an intensity that strongly depends on the incident and viewing angles. The SPR behavior of metal NPs has been deliberately applied by ancient artisans to manufacture mysteriously aesthetic glass. One of the most spectacular examples is Lycurgus Cup, which exhibits a translucent ruby color in transmittance while an opaque greenish-yellow color in reflection as a result of the SPR behavior of gold/silver alloy NPs embedded in the glass.<sup>9</sup> A variety of transition metal NPs have been manufactured to evaluate the use of their SPRs in the fabrication of novel nanoplasmonic devices for controlling electrons and light.<sup>9-12</sup> However, gold (Au) NPs remain the workhorse in literature due to their excellent chemical stability, strong SPR absorption bands in the visible light spectrum, easy control of the synthesis of NP with various sizes and shapes,

with fairly narrow distribution, and easy surface modification.<sup>13</sup> Spherical Au NPs display a single, sharp absorption band due to the excitation of so-called dipole SPR,<sup>14,15</sup> where the entire charge distribution of the particle oscillates at the frequency of the incident electric field (Fig.1A and 1C). As the size of the spherical Au NPs increases, multiple absorption bands appear due to quadrupole and other higher ordered SPRs (Fig.1A and 1C).<sup>15</sup> For Au NPs with non-spherical shapes, other modes of SPR arise, because the charge distribution on the NP surfaces becomes anisotropic and in turn changes the restoring force. Gold nanorods (Au NRs) are the typical model to testify how the optical SPR properties of elongated Au NPs are dependent on their aspect ratios and dimensions. Typically, the SPRs of Au NRs in a solution result in two absorption bands (Fig.1B).<sup>16</sup> The SPR resonance at the longer wavelength, referred to as longitudinal SPR, is associated with the surface plasmon electron oscillations along the NR length, while that at the shorter wavelength, referred to as transverse SPR, is associated with the surface plasmon electron oscillations along the NR width.<sup>17-19</sup> The positions of the two SPR bands depend on both the aspect ratios and the absolute dimensions of Au NRs.

Recent theoretical studies<sup>20-25</sup> reveal that when multiple metal NPs are assembled together, the total absorption cross sections will be increased for better SPR transduction, and new SPR properties are generated, which are not present in single particles otherwise. SPR coupling is one of the most exciting features for metal NP assemblies. When two or more metal NPs are brought in close proximity on the order of nanometers, the surface plasmon oscillating electric fields of individual NPs can be coupled to new resonances localized in the gaps between the NPs<sup>21,22</sup> and following the principles of molecular hybridization.<sup>26</sup> When the interparticle coupling is effectively controlled, extremely high local electric fields can be generated, which are known as hotspots.<sup>23-25,27,28</sup>

<sup>a</sup>State Key Laboratory of Crystal Materials, Shandong University, Jinan, 250100, P. R. China. E-mail: hbxia@sdu.edu.cn

<sup>b</sup>Ian Wark Research Institute, University of South Australia, Adelaide, SA 5095, Australia. E-mail: Dayang.Wang@unisa.edu.au

<sup>†</sup>These authors contributed equally to this work

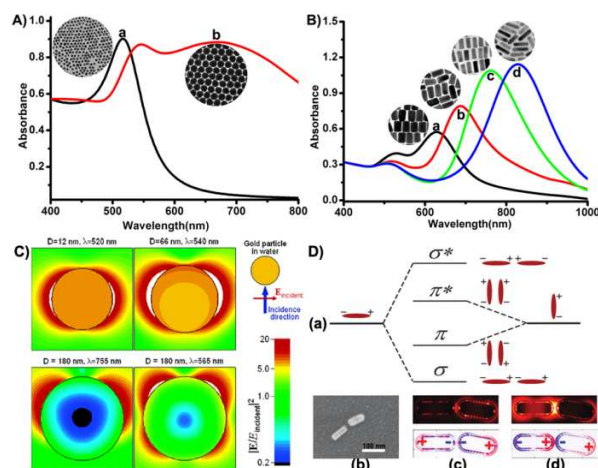


**Fig. 1** (A) Extinction spectra and TEM images of Au NPs with different sizes: (a) 12 nm and (b) 330 nm. (B) Extinction spectra and TEM images of Au NRs with different aspect ratios: 1.8 (a, black curve), 2.6 (b, red curve), 3.3 (c, green curve) and 4.0 (d, blue). (C) Near field enhancement at spherical Au NPs with different sizes in water under the illumination at their corresponding SPR wavelengths. Reproduced from ref. 15 with permission from the American Chemical Society. (D) Plasmon hybridization analogy to molecular orbital theory: the coupled longitudinal plasmon modes of end-to-end and side-by-side assembled Au NR dimers (a). SEM image of the end-to-end Au NR dimer (b). FDTD-calculated electric field enhancement (upper) and charge distribution (lower) at the maxima for the short (secondary) and long (primary) wavelength scattering peaks, respectively (c and d). Reproduced from ref. 26 and 29 with permission from the American Chemical Society.

For instance, when two Au NRs are assembled into a bent-touching dimer in an end-to-end configuration with an approximate separation of 12 nm, the anti-parallel and parallel coupling of their longitudinal dipole modes arise, particularly the latter yields hotspot in the gap space between the NRs (Fig. 1D).<sup>29</sup>

In this context, the directed self-assembly of metal NPs into tailored architectures with defined spatial configuration of the constituent NPs, which is paramount for the manipulation of the interaction of the NPs with light of wavelength that significantly exceeds their dimensions, is drawing exponentially increased attention in the research of nanoscience. This review, focuses on the directed self-assembly of Au NPs into one dimensional chains in solution as well as in their plasmonic behavior. In the following sections, firstly, recent experimental advances in the synthesis of monodisperse Au NPs with defined shapes are highlighted, which are the key building blocks for NPs self-assembly. The second section provides an overview of current development in the direct self-assembly of Au NPs into linear NP chains, which focuses on the understanding of the underlying thermodynamics and kinetics to govern NP self-assembly. The third section describes the plasmonic behavior of as-prepared NP chains. The review concludes with a summary and personal outlook of future directions in the field of plasmonic NP self-assembly.

## 2. Directed self-assembly of Au NPs

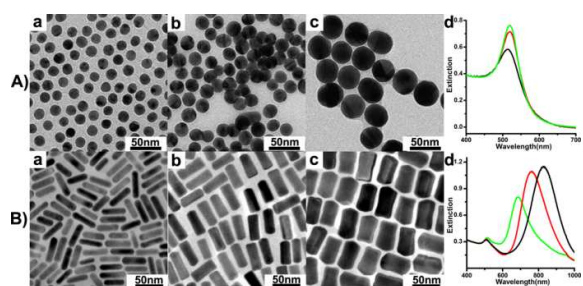


**Fig. 2** (A) TEM images (a to c) and extinction spectra (d) of Au NPs with different sizes: 12 nm (a, black curve), 25 nm (b, red curve) and 36 nm (c, green curve). (B) TEM images (a to c) and extinction spectra (d) of Au NRs with different aspect ratios: 2.0 (a, black curve), 2.5 (b, red curve), and 3.3 (c, green curve). Reproduced from ref. 14 with permission from the American Chemical Society.

### 2.1 Synthesis of monodisperse Au NPs of different shapes

Controlling the morphology (shapes, sizes, etc) of Au NPs is crucial for the experimental study and tailoring of the plasmonic behavior of individual NPs and their self-assembly. Moreover, the narrow size and shape distribution is also essential for directing NPs to self-assemble into uniform structures in high yield, since a tiny variation in size and shape results in large differences in interaction between the constituent NPs and thus in non-uniform NP self-assembly in solution. In this context, a great deal of effort is still put in development of new strategies for the synthesis of monodisperse, quasi-spherical Au NPs with different sizes. Currently, the simplest way to synthesize monodisperse, quasi-spherical Au NPs is still the reduction of auric chloride acid ( $\text{HAuCl}_4$ ) by sodium citrate in water, which was established by Turkevich et al. in early 1950's.<sup>30</sup> When the Turkevich method is applied to produce Au NPs larger than 20 nm by reducing the molar ratio of citrate to auric acid, known as the Frens method, the NP size distribution becomes significantly broader and the NP shapes become noticeably elongated or even irregular.<sup>31</sup> Yang et al. recently reported a significant but less recognized impact of citrate on the growth of Au NPs in Turkevich method,<sup>32</sup> the sodium citrate buffer effect. They found that adding the citrate to auric acid may cause temporary pH alteration in the reaction media, which, in turn, alters the nature of the auric acid and thus its reactive activity. Xia et al. modified the conventional protocol for the Turkevich method to prepare monodisperse, quasi-spherical Au NPs with sizes varying from 12 nm to 36 nm (a, b and c in Fig. 2A). Although the SPR maxima of the as prepared Au NPs strongly depends on the NP size, the blue-shift in the maxima is not significant, due to their truly quasi-spherical shape (d in Fig. 2A).<sup>14</sup> They mixed sodium citrate, auric acid and a trace amount of silver ions in water and subsequently injected into boiling water. The pre-mixing not only minimizes the pH buffer effect of citrate on the reactive activity of auric acid, but also enables temporal separation of nucleation and growth steps, because a low reaction temperature (in this case, room temperature for mixing) is favorable for citrate reduction of Au (3+) into Au (1+) for nucleation, while a high reaction temperature (in boiling water) significantly slows down the autocatalytic process of Au (1+) to Au (0) for Au NP growth.

According to the well-known LaMer model,<sup>33</sup> this temporal separation between nucleation and growth steps should be the key factor accounting for the formation of monodisperse, quasi-spherical Au NPs. To date, the seeded growth method<sup>34-37</sup> in which pre-formed small NPs act as both catalysts and nucleation sites (seeds) for reduction and deposition of metal ions, is the widely used method for synthesis of monodisperse, quasi-spherical Au NPs with sizes bigger than 12 nm. The groups of Murphy and Liz-Marzan reported the successful seeded growth of monodisperse, quasi-spherical Au NPs with sizes range from 12 nm to 180 nm by using cetyltrimethylammonium bromide (CTAB) as stabilizing agent to control NP growth.<sup>15,34</sup> Puntès et al. reported a kinetically controlled seeded growth strategy for the synthesis of monodisperse citrate-stabilized Au NPs of sizes from 10 nm up to ~200 nm, via the reduction of auric acid by sodium citrate.<sup>38</sup> The obtained NPs are highly monodisperse (with a narrow size distribution) and with uniform quasi-spherical shape, as compared to the particles produced by the Frens method. The main disadvantage of the method reported by Puntès et al., is that the growth of the seeds to the desired size is not achieved in one step. Thereby, the synthesis of larger particles needs stepwise growth of Au NPs with intermediate sizes. However, the main advantage of the method of Puntès et al. is that it obviates the use of CTAB, which strongly binds to the Au NP surface and restricts the possibility of further functionalization. Wang et al. reported a facile, fast, surfactant-free method for the synthesis of quasi-spherical Au NPs with a size range from 12 nm to 230 nm, using hydrogen peroxide as a reducing agent.<sup>39</sup> Au NPs with sizes below 6 nm can be prepared by using thioether- and thiol-functionalized polymer as ligands<sup>40</sup> or by aging an oleylamine-H[AuCl<sub>4</sub>] toluene solution in the presence of cobalt nanoparticles as a sacrificial template.<sup>41</sup>

Advancements in the last 15 years, have given rise to a number of reliable methods for the synthesis of Au NRs. Above all, the CTAB-assisted protocol developed by the group of Murphy, enabling the synthesis of monodisperse Au NRs with a defined aspect ratio in high yield and varied spectra (Fig. 2B).<sup>36,37,42-45</sup> Recently, Xia et al. succeeded in the direct synthesis of monodisperse Au NPs with cubic, trisoctahedral, and concave shapes in high yield.<sup>46</sup> This has enabled the establishment of better shape-SPR correlation for Au NPs,<sup>46</sup> and has also provided new building blocks with a variety of shapes that can be used to create novel plasmonic nanostructures.

## 2.2 In situ monitoring of NP chain growth in solution

Up to date, many studies of NP self-assembly rely on the structural characterization with the aid of transmission electron microscopy (TEM), which may largely be distorted by the drying effect during TEM sample preparation. Due to the unique plasmonic character of Au NPs, the self-assembly process of Au NPs can be monitored *in situ* by ultraviolet (UV)-visible spectroscopy.<sup>47-49</sup> Wang et al. calculated the SPR absorption of Au NP chains under excitation with light polarized, parallel to the longitudinal direction of the chain (Fig. 3).<sup>50</sup>

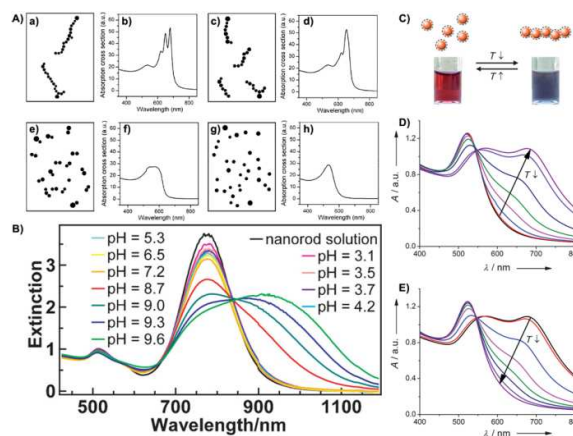


**Fig. 3** (A) Schematic models of the chains comprising of Au NPs of different numbers and their calculated extinction spectra under excitation with light polarized parallel to the longitudinal direction of the chain. Reproduced from ref. 50 with permission from the American Chemical Society. (B) Extinction spectra of Au NR solutions recorded at different pH values. (C) Color switching of Au NPs dispersion in response to temperature changes, (D) the extinction spectra of a typical Au NP dispersion with temperature decreasing, and (E) with temperature increasing, respectively. Reproduced from refs. 48 and 49 with permission from the Wiley Interscience.

Their calculations indicate that the transverse SPR of the NP chains at 520 nm remains unchanged, while the longitudinal SPR in the wavelength range of 600-800 nm blue-shifts, which evolves from a shoulder peak near the transverse SPR band to a pronounced band consisting of three peaks with the increase of the NP chain length. The calculated spectra of the chains of Au NPs are consistent with the experimental spectra. In addition to TEM observation, the variation of the longitudinal SPR band observed provides a useful measure to *in situ* monitor self-assembly of Au NPs into chains.

## 2.3 Directed self-assembly of Au NPs to chains

Strategies for the directed self-assembly of Au NPs into chains in solution, reported in current literature, can be divided into two categories: template-assisted self-assembly and template-free self-assembly. The latter relies on a deliberate balance of the interactions, between the NPs, mainly non-covalent interactions, which can be adjusted by the nature of multifunctional thiol molecules, biological molecules, or polymers anchored on Au NPs. In this review the focus is mainly on template-free, non-covalent self-assembly of Au NPs into chains, although a brief overview of state-of-the-art of template-assisted self-assembly is included.

### 2.3.1 Growth of Au NP chains via template-assisted self-assembly

A host of efforts have been devoted to the use of one-dimensional (1D) molecular or nanoscale templates such as carbon nanotubes,<sup>51</sup> block copolymer micelles,<sup>52</sup> and Au nanowires (NWs)<sup>53</sup> to guide the self-assembly of Au NPs into 1D NP assemblies. For instance, pre-formed Au NWs can induce the assembly of NPs and NRs into ordered arrays in solution. Carefully adjusting the distances between the NPs yield distinct optical response of the NP/NW films, which can be easily discerned by the naked eye.<sup>53</sup>

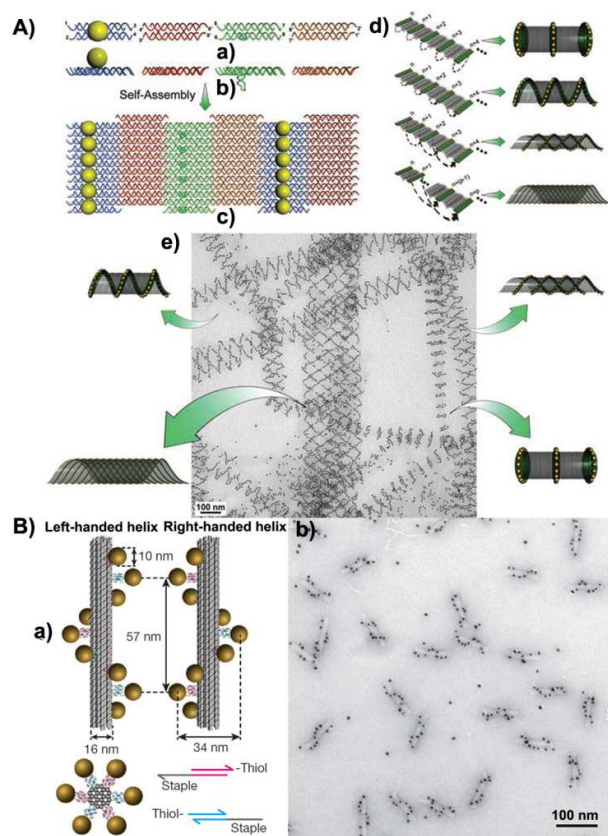


**Fig. 4** (A) Scheme of a DNA tile system for the formation of a variety of tubular structures carrying 5-nm Au NPs (a to d in Fig. 4A) and TEM image of different tube conformations composed of Au NPs (e in Fig. 4A). Reproduced from ref. 58 with permission from the American Association for the Advancement of Science. (B) Assembly of DNA origami Au NP helices (a in Fig. 4B) and TEM image of assembled left-handed nanohelices composed of Au NPs (b in Fig. 4B). Reproduced from ref. 61 with permission from Nature Publishing Group.

Recently, the group of Chen reported a new appealing strategy based on the microstructures of polycrystalline ice. By simply freezing the aqueous solution of NPs, Chen et al. obtained unbranched, ultra-long chains with uniform cross sections, whose stability can be strengthened by polymer encapsulation. Due to its unique molecular recognition capability and structural versatility, DNA has been widely exploited as the template to control the complexity and regularity of NP self-assemblies.<sup>55–57</sup> 1D spiral chains, double helices and even nested spiral tubes of Au NPs were constructed by controlling the locations of stem loops on double-crossover DNA tiles, and size-dependent steric and electrostatic repulsion effects, due to the incorporation of Au NPs (Fig. 4A).<sup>58</sup> Based on electrostatic interactions between the cationic ligand coating of Au NPs and the anionic backbone of DNA, the NPs were attached onto the backbones of  $\lambda$ -DNA templates, resulting in the formation of regularly spaced linear chain-like NP structures.<sup>59</sup> DNA nanotubes, consisted of large and small capsules alternatingly associated along the tubes, were used for size-selective loading of Au NPs to form linear ‘nanopeapod’ structures, which could be actively released upon addition of specific DNA strands.<sup>60</sup>

The DNA origami method is widely used to fabricate helical NP chains,<sup>61</sup> where hundreds of rationally designed ‘staple’ oligonucleotides are hybridized to long single-stranded DNA scaffolds and then arranged into specific two- or three-dimensional structures. Using this technique, discrete chiral helical chains of Au NPs were formed by hybridizing DNA ligands with Au NPs attached to pre-formed DNA scaffolds (Fig. 4B).

### 2.3.2 Growth of Au NP chains via template-free directed self-assembly

#### 2.3.2.1 Directed self-assembly of Au NPs coated with small thiol molecules

Molecules containing thiol groups are widely used to functionalize Au surfaces due to the formation of strong semi-covalent Au–S bonds.<sup>62</sup> The specific recognition between thiol-terminated biological molecules anchored on Au NPs has been often utilized to couple the Au NPs or NRs into dimers, trimers, and other oligomers. Murphy et al. pioneered the work of coupling Au NRs into end-to-end assemblies by specific bindings between biotin and streptavidin selectively modifying the ends of the Au NRs.<sup>63</sup> Despite the success in self-assembly directed by specific recognition between elegant biological ligands, the simplest way to control self-assembly of Au NPs is the judicious control of the electrostatic repulsion and the electric dipoles between the Au NPs. Mann et al. reported the formation of chain-like structures of Au NPs where the neutral thiol ligand, 2-mercaptoethanol, (MEA, HS(CH<sub>2</sub>)<sub>2</sub>OH) was used to replace ionic citrate molecules thus reducing the electrostatic repulsion (a in Fig. 5A).<sup>64</sup> Due to spatial partitioning of the mixed capping ligands of MEA and citrate, the electrostatic repulsion between the Au NPs was progressively reduced; and the stability of the electric dipole associated with the charge separation on the NP surface was potentially enhanced. It is clearly observed that the cross-linking points in chain networks of Au NPs are the big or small NPs not the ones of intermediate sizes. The results of Mann et al. indicated that the shape and size uniformity of Au NPs is essential for the formation of uniform, linear chains without branches. As-prepared chain networks of Au NPs enabled one-dimensional plasmonic coupling, thus opening a unique opportunity to experimentally study the optical waveguide performance in subwavelength metallic structures. Correlating with these results, theoretical simulation of far-field extinction spectra of the as-prepared chain networks of Au NPs, also showed a strong SPR coupling of adjacent non-contacting NPs. Heat was efficiently generated by exciting the longitudinal coupled mode of neighboring NPs and confined near the NP chain networks (b to e in Fig. 5A).<sup>65</sup> The chain networks of Au NPs were converted *in situ* into continuous and crystalline metallic bead strings after the removal of capping ligands via oxygen plasma cleaning.<sup>66</sup> Interestingly, their electron energy loss spectroscopy (EELS) spectra after fusion (b in Fig. 5B) present a second low-energy peak besides its maximum peaks at 1.11 (position I) or 1.61 eV (position II). The corresponding EELS maps (c to e in Fig. 5B) illustrated the spatial distribution of the three SPR modes along the NP loop, which were in good agreement with simulations maps (f to h in Fig. 5B).

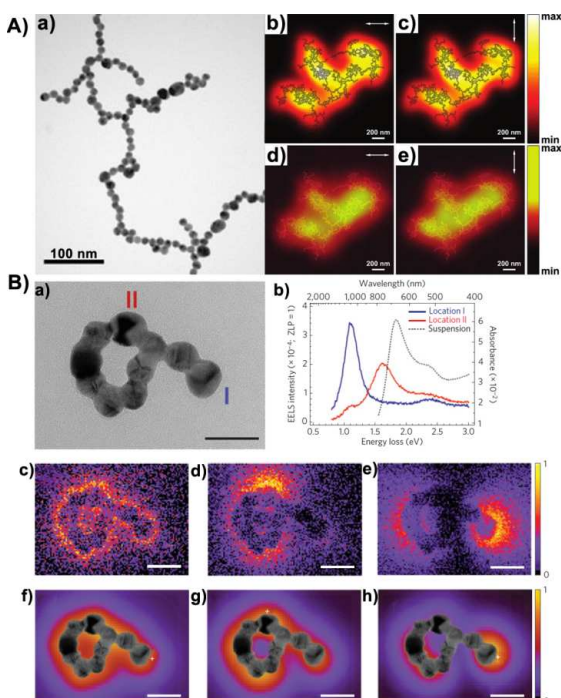


**Fig. 5** (A) TEM image (a in Fig. 5A) of a self-assembled NP chain network. Calculated (b and c in Fig. 5A) and experimental images (d and e in Fig. 5A) are overlaid with the positional network particle map and the SEM image of the NP networks, respectively. Reproduced from refs. 64 and 65 with permission from Wiley Interscience and the American Chemical Society, respectively. (B) Spatial and spectral characterization of plasmon-mediated electron energy loss in the vicinity of a fused chain of Au NPs. Scale bars are 50 nm. Reproduced from ref. 66 with permission from Nature Publishing Group.

A larger chain networks of Au NPs comprising several loops and chains of fused NPs was also studied. The EELS map of the transverse SPR mode recorded at 2.40 eV confirmed its extreme and homogeneous confinement along the edge of the entire structure. In addition, each sphere showed a dipolar polarizability in the computed EELS map.<sup>66</sup>

When pH-sensitive thiols such as 3-mercaptopropionic acid, glutathione, and cysteine were preferentially bound to the ends of CTAB-stabilized Au NRs, the Au NRs could reversibly self-assemble into end-to-end NR chains upon the environmental pH change.<sup>67</sup> When both the end and side surfaces of CTAB-stabilized Au NRs were modified by for instance 11-mercaptoundecanoic acid, the adjustment of environmental pH guided the NRs to reversibly self-assemble into either end-to-end or side-by-side chains.<sup>68</sup> Liz-Marzan et al. shed some light in explaining the mechanism through which Au NRs modified with bifunctional linking molecules preferentially assemble in an end-to-end fashion. This chained self-assembly of the Au NRs was due to a pH-controlled hydrogen-bonding between protonated and unprotonated groups of the linking molecules.<sup>69</sup> In addition to the environmental pH, surface modification of Au NPs with other dipictioliol ligands may lead to reversibly guide self-assembly of the NPs into chains by using other stimuli.

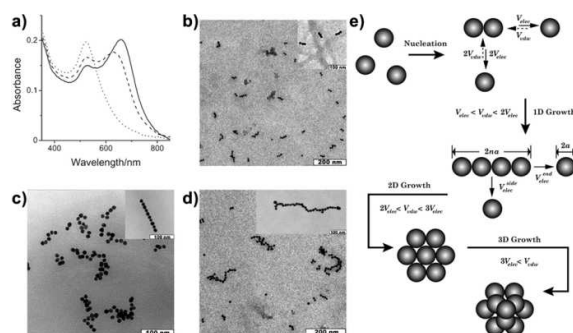


**Fig. 6** Extinction spectra (a) and TEM images (b–d) of Au-NP chains obtained using the different water–acetonitrile volume ratios: (b) 1:1(—), (c) 1:2(---), and (d) 1:3(—). Insets are the corresponding TEM images with high magnification. (e) Schematic representation of self-assembly process of charged particles endorsed by a balance between isotropic long-range electrostatic repulsion and isotropic short-range van der Waals attraction between the particles in the presence of short-range anisotropic dipolar attraction forces. Reproduced from ref. 76 with permission from the Wiley Interscience.

For instance, thiol-modified crown ethers, peptides, N,N,N-trimethyl(11-mercaptoundecyl)ammonium chloride among others have been used to control self-assembly of Au NPs by adjusting the ionic strength and the nature of metal ions in solution.<sup>70–74</sup> Furthermore, the plasmonic behavior alteration of Au NPs associated with reversible self-assembly in response to external stimuli-responsive also provided a ultrasensitive way to sense a tiny change in the surrounding environment of the NPs, useful for the fabrication of ultrasensitive sensors.<sup>75</sup>

Recently, Zhang and Wang developed a consistent model, based on the Derjaguin–Landau–Verwey–Overbeek (DLVO) theory, to describe how charged NPs can self-assemble into chains and how the length of as-prepared Au NPs is correlated with the electrostatic interaction between the NPs (Fig. 6).<sup>76</sup> They took into account the electrostatic repulsion potential ( $V_{elec}$ ), the van der Waals attraction potential ( $V_{vdW}$ ), and the dipolar interaction potential ( $V_{dipole}$ ) to estimate the colloidal stability of monodisperse spherical Au NPs. In addition, they also estimated the electrostatic repulsion potential at either end of a NP chain in the proximity of a NP,  $V_{elec}^{end}$ , and that between the chain side and a neighboring NP,  $V_{elec}^{side}$ . Based on the modified model of electrostatic interaction between elongated objects,  $V_{elec}^{end}$  and  $V_{elec}^{side}$  can be correlated with the surface density ( $\rho$ ) and the radii ( $a$ ) of the NPs and the number ( $n$ ) of NPs composing the NP chains as below:<sup>76</sup>

$$V_{elec}^{end} = \rho \cdot A \cdot \ln 2na \quad (n > 2) \quad (1)$$

$$V_{elec}^{side} = 2\rho \cdot A \cdot \ln na \quad (n > 2) \quad (2)$$

This underlines that  $V_{elec}^{end}$  is relatively weaker than  $V_{elec}^{side}$ , which effectively prevents the attachment of the NPs into the sides of newly formed NP chains, thus warranting the self-assembly of charged NPs into chains and the high colloidal stability of the NP chains. At equilibrium of NP self-assembly to chains, the total energy is zero. Thus, the value of  $V_{elec}^{end}$  should be equal to the sum of  $V_{vdW}$  and  $V_{dipole}$ . Accordingly, the number ( $n$ ) of NPs composing the chain can be calculated as follows:

$$n = \frac{\exp[-(V_{\text{vdw}} + V_{\text{dipole}}) / \rho A]}{2a} \quad (3)$$

As such, the number of NPs per chain is controlled by the surface charge density, which can be tuned by the ionic strength and dielectric contact of the surrounding aqueous environment (Fig. 6).

### 2.3.2.2 Directed self-assembly of Au NPs coated with polymer brushes

Due to significant development in new polymerization strategies,<sup>77</sup> a variety of polymer brushes, especially stimuli-responsive polymer brushes, can be anchored on Au NPs. When polymers are coating the surface of the Au NPs, the interactions between NPs cannot be reasonably explained by means of the classic DLVO forces, in this case, the steric repulsive and solvophobic attractive forces have to be taken into account. Kumacheva et al. reported the directing self-assembly of polymer coated Au NRs by deliberately adjusting the location of the polymer ligands, the volume ratio of the NRs to the polymer ligands, and the solvent selectivity of the polymer ligands (Fig. 7).<sup>78-82</sup>

They selectively tethered hydrophobic homopolymers on both ends of hydrophilic, CTAB-stabilized Au NRs, which were considered as nanoscale amphiphilic ABA triblock copolymers. By selectively changing the composition and ratios of the solvents for the stabilizing molecules (polystyrene and CTAB), Au NRs were assembled into rings, nanochains, bundles, nanospheres and bundled nanochains.<sup>78</sup> It was clearly observed that the size distribution of final Au NR ensembles was broad, evoking the wide distribution of number-average molecular weight of polymers or oligomers derived from condensed polymerization. Kumacheva<sup>79</sup> et al. reported a molecular copolymerization approach to describe the kinetics and the length of as-prepared Au NRs (Fig. 7). The approach was also extended to direct different NRs, for instance Au and Pd NRs to self-assemble together into composite chains, reminiscent of co-polymers.

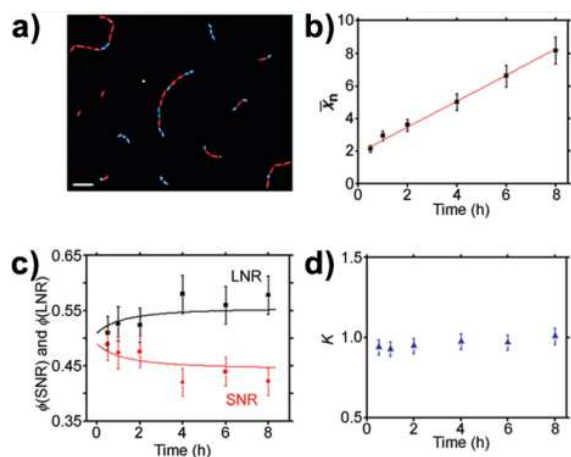


Fig. 7 Co-assembly of short and long Au NRs. STEM image of short and long Au NRs processed by Matlab program (a), their average degree of polymerization (b), their fractions in the chains (c), and their microheterogeneity coefficient (d) with self-assembly time. Reproduced from ref. 79 with permission from the Wiley Interscience.

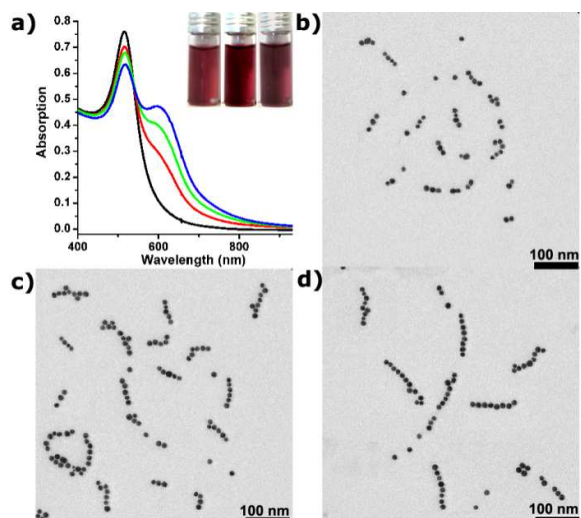


Fig. 8 Evolution of the extinction spectrum (a) of an aqueous dispersion of Au12@C-PDMA NPs with the pH values of the medium: 4.0 (black curve) to 3.5 (red curve), 3.0 (green curve), and 2.5 (blue curve). The inset shows digital photographs of the corresponding dispersions at pH 3.5 (left), 3.0 (middle), and 2.5 (right). TEM images (b–d) of Au12@C-PDMA NP chains obtained at (b) pH 3.5, (c) 3.0, and (d) 2.5. Reproduced from ref. 47 with permission from the Wiley Interscience.

Kumacheva et al. also demonstrated how the competition between solvophobic attraction forces and electrostatic repulsion forces leads to transitions between chain-like and globular structures of charged polystyrene-coated Au NPs.<sup>80</sup> Further, they quantitatively assessed the kinetics and statistics of the self-assembly of Au NRs based on the models of reaction-controlled step-growth polymerization, enabling the prediction of the possible architectures of linear, branched, and cyclic assembled Au NRs, their aggregation numbers and size distributions.<sup>81</sup>

Xia et al. coated monodisperse, quasi-spherical Au NPs with pH-sensitive polymer brushes, poly[[2-(dimethylamino)ethyl] methacrylate] (PDMA). These pH-sensitive hairy Au<sub>n</sub>@C-PDMA NPs were reversibly self-assembled into chains in response to the stepwise adjustment of the environmental pH value (Fig. 8).<sup>47</sup> Accordingly, the length of as-prepared NP chains is determined by the environmental pH value and depends little on the size of the NPs, whereas according to Equation 4, the number of NPs per chain decreases as the NP size increases.<sup>47</sup>

$$n = \frac{1}{d} + \frac{[6(-V_A^{\text{end}}) / \rho\pi]}{d^3} + \frac{[6(-V_A^{\text{end}}) / \rho\pi]^2}{2!d^5} + \frac{[6(-V_A^{\text{end}}) / \rho\pi]^3}{3!d^7} + \dots \quad (4)$$

Using the pH-sensitive polymer coating, Xia et al. also succeeded in the coupling of as-prepared chains made of differently sized NPs into linear composite chains with configurations reminiscent of those of di- or triblock copolymers. The configuration of as-prepared composite chains was determined by the size ratio of large to small NPs, which could be assessed based on the following equation.<sup>47</sup>

$$\sqrt{r} + \frac{1}{\sqrt{r}} \leq 2 + C \quad (5)$$

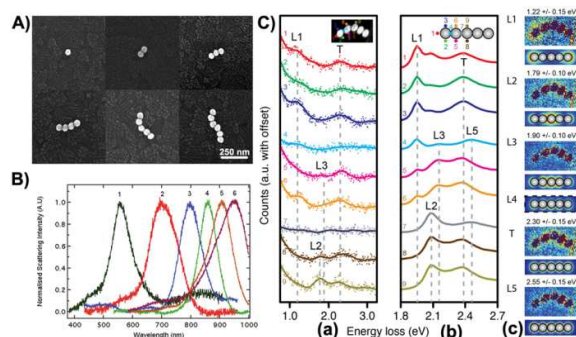


**Fig. 9.** (A) SEM images of self-assembled chains containing different NP numbers (from 1 to 6). The mean diameter of Au NPs is 64 nm. Interparticle spacings are estimated at 1 nm. (B) Normalized spectra of the corresponding NP chains in Fig. 9A. (C) Experimental (a) and modeled (b) EELS spectra of the 5-NP chain taken at different locations indicated by the numbers in the insets. (c) Experimental (upper) and modeled (lower) EELS maps of the (L1)  $l = 1$ , (L2)  $l = 2$ , (L3)  $l = 3$ , (T) transverse (L4)  $l = 4$  (model only, calculated using the Drude model), and (L5)  $l = 5$  modes present within the 5-NP chain. Au NPs used in this work have diameters of 45 nm. Reproduced from refs. 84 and 85 with permission from the American Chemical Society.

Unlike the approach reported by the group of Kumacheva, in which solvophobic forces drove Au NRs into chains with fairly broad length distribution, the Au NP chains produced by Xia et al. have a fairly narrow distribution of the chain length and especially in the number of NPs per chains. This underlines that reversible self-assembly of pH-sensitive Au NPs is arrested in the chain structures with a minimal thermodynamic potential at a given pH, since both NPs and newly formed NP chains remain colloidally stable. In contrast, if the self-assembly of NPs is not reversible, the NPs may eventually aggregate together and participate driven by solvophobic forces, as reported in the work of Kumacheva. The NPs self-assembly may be kinetically frozen to the chains with a broad length distribution.

### 3. Nanoplasmonics applications

Although Au NPs have one plasmon mode, when they self-assemble into chains, different collective plasmon modes appear and follow the principles of molecular hybridization.<sup>83-85</sup> The plasmon modes of individual Au NPs can be hybridized to form a lower energy bonding plasmon mode and a higher energy anti-bonding plasmon mode (Fig. 1D). Alivisatos,<sup>83</sup> found that for the plasmon coupling of homodimers (Ag-Ag NPs), the in-phase mode is optically allowed, whereas the out-of-phase mode is dark, due to the cancellation of the equivalent dipole moments. For the plasmon coupling of heterodimers (Ag-Au NPs), the bonding modes were red shifted with respect to the Au NP plasmon resonance and the anti-bonding modes blue shifted with respect to the Ag NP plasmon resonance. Due to the geometrical configuration of Au NP (or Au NR) chains, coupled Au NPs exhibit extremely rich spectral responses. Mulvaney et al. reported a red-shift of the SPR with the NP chain length increasing when the linear chains are consisting of six or less Au NPs with 1 nm interparticle spacing (Fig. 9A and 9B).<sup>84</sup> Recently, they further demonstrated

that a chain containing  $N$  NPs can accommodate at least  $N$  experimentally observable modes, in addition to the transverse mode. When the chain length increases by the addition of one more Au NP to the chain, the new  $N + 1$  mode appears as the highest energy mode (L5), while the existing modes lower their energy and eventually decay to zero as they delocalize along the chain (Fig. 9C).<sup>85</sup> The plasmon coupling of Au NPs (or Au NRs) also provides much stronger electric field enhancement; increased by many orders of magnitude. Accordingly, minute changes in the local environment can be amplified significantly to enable ultrasensitive detection. These unique properties offer great potential in a variety of applications, such as highly sensitive biological and chemical sensors.<sup>86,87</sup> The location of hotspots is largely determined by the mutual orientation of NPs in chain-like structure, interparticle distance, and the aggregation number of the self-assembled nanostructures, characteristics that are easily controlled during solution-based self-assembly of the NPs.

Due to their larger electric field enhancement and polarizability, Au NRs are better candidates, compared with their spherical counterparts, to be used for plasmonic sensing. For instance, a new strategy for plasmonic sensing was designed based on the spectral shift due to the plasmon coupling of Au NRs close to each other but not contact. Kotov et al. described the successful use of Au NRs for detection of a pervasive environmental toxin, microcystin-LR, based on the side-by-side and end-to-end NR self-assemblies.<sup>88</sup> Kumacheva further investigated the relationship between the dynamic structural characteristics of self-assembled chains of Au NRs and their ensemble-averaged SERS (Surface Enhanced Raman Spectroscopy) properties resulting from the controlled generation of plasmonic electromagnetic hot-spots (Fig. 10a).<sup>89</sup> They established a direct relationship between the extinction and SERS properties of the NR chains; the SERS intensity was not monotonically dependent on the NR number per chain, but it nearly followed the extinction product, which is defined as the product between the extinctions of the assemblies at the excitation and Raman scattering wavelengths.<sup>89</sup>

Short Au NP chains (dimer or trimer) were also used to study the enhancement factor of "hotspots" resulting from strong plasmon coupling within the gaps between the NPs. It was demonstrated that the ensemble-averaged SERS enhancement factor from spatially isolated colloidal NP chains was improved 16 and 87 times than that of single NPs.<sup>90</sup> Lim et al. also demonstrated that hotspots were generated between NP dimers of DNA-conjugated Au NPs, in which DNA was used to trap a dye molecule within the hot spots (Fig. 10b).<sup>91</sup> Moreover, the interparticle gap between Au NP dimers were decreased by formation of a silver shell on Au NPs. This led to the achievement of single molecule detection. Recently, the group of Chen reported a less known effect of hotspots which may cause trapped analytes to change their molecular orientation and in turn leading to pronounced changes in their SERS fingerprints. When the SERS analytes were introduced into the hotspots formed in the assembly of linear Au NRs chains, a large SERS enhancement was observed, particularly

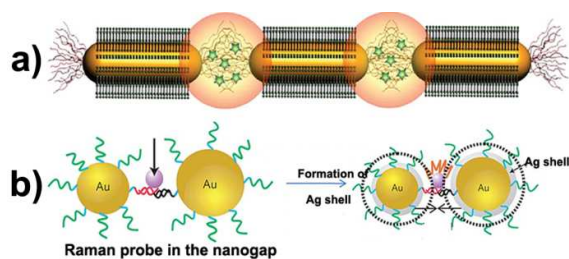


**Fig. 10** (a) Hot spots formed in between the ends of Au NRs by end-to-end NR assembly in the presence of the Raman probe oxazine 720. Reproduced from ref. 89 with permission from the American Chemical Society. (b) Hot spots generated between NP dimers of DNA-conjugated Au NPs. Reproduced from ref. 91 with permission from Nature Publishing Group.

for some weak or inactive SERS modes that were not present in the original spectrum before the formation of hotspots.<sup>92</sup>

Chiral plasmonics has received increasing interest as an emerging and hot research topic due to the combination of NPs and chiral molecules, which provides new opportunities not only in optics but also in biology.<sup>93</sup> Many types of plasmonic NP chains have exhibited plasmonic circular dichroism (CD) features (amino acids,<sup>94</sup> single-stranded DNA,<sup>95</sup> and DNA bundles<sup>61</sup>). The coupled plasmon waves between Au NPs in helical DNA can propagate along a helical path and cause increased absorption of those components of the incident light, thus leading to the bisignate appearance of the CD signals from the isotropic nature of Au NPs.<sup>61</sup> These experimental spectra were in good agreement with theoretical calculations based on classical electrodynamics. The generation of CDs at other wavelengths can be achieved by replacing Au NPs with Au@Ag NPs with Ag shell of 3 nm. Moreover, this method was also applied for sensing toxins, microcystin-LR, and a cancer biomarker, prostate-specific antigen, using chiral heterodimers made of Au and Ag NPs.<sup>96</sup> In this context, the preparation of chain-like Au NPs with different chiral molecules can be rather useful in rational design and tunable handedness, color and intensity of the optical response.

#### 4. Conclusion and outlook

The organization of metal NPs into plasmonic chains is one of the most appealing themes in the research of NP self-assembly. Inspired by molecule synthesis and self-assembly, “molecular mimetic” approaches are proposed to guide NP self-assembly.<sup>97</sup> Linear chains, consisting of identical or different metal NPs in terms of the size, shape, and chemical nature can be regarded as plasmonic homopolymers,<sup>98</sup> or copolymers.<sup>79</sup> The classic theory of condensation polymerization can be applied to predict the behavior of kinetic-driven self-assembly of NPs to chains and the chain length distribution. On the other hand, classic and extended DLVO theories allow the prediction of the behavior of thermodynamic-driven self-assembly of NPs into uniform chains and the tailoring of the chain length via the balance of the interactions between the NPs.<sup>99</sup> Self-assembly of metal NPs

may also pave the way for fundamental studies of chemical concepts in a retroactive manner. For example, the chains of Au NRs with a wide distribution of aggregation numbers, bond angles, chain conformations or varying compositions give simultaneous access to molecular interactions and molecular self-assembly behaviors at nanoscale.<sup>81</sup> For instance, the revealed effect of the large/small NP size ratio on the configuration of the composite chains may have strong implication in condensation of amino acids into peptides and self-organization of peptides.<sup>47</sup>

It is clear that the future research in the field of self-assembly of metal NPs will focus on the better understanding and manipulation of the interactions between Au NPs in order to tailor more sophisticated spatial configurations of NP self-assemblies. This will be crucial for fundamental studies of the correlation of the surface plasmonic properties of metal NP self-assemblies such as SERS, scattering, extinction, Fano resonance, or circular dichroism with their structural features. Till now, however, most of the published articles report plasmonic properties of chain-like structured Au NPs (or NRs), though silver NPs have largest quality factor across most of the spectrum from 300 to 1200 nm.<sup>100</sup> This limitation can be partly attributed to the challenges in the synthesis of Ag NPs with narrow size and shape distribution.<sup>101,102</sup> In this context, the mechanism governing growth of Ag NPs, as well as other transition metal NPs, will need to be revisited to develop novel and reliable protocols to produce NPs with defined but varied sizes and shapes. This will enable us to incorporate different metal NPs into plasmonic copolymers with tailored surface plasmon models.

Currently, self-assembled plasmonic nanostructures are still mainly used as chemical and biochemical sensors. Enhancement of electric field in hot spots can control many processes ranging from the precise local delivery of heat to enhanced generations of excited states and electron- and hole-transfer processes that can contribute to photo-redox processes. Chiral plasmonics is an emerging research field that utilizes chiral organization of metal NPs with chiral molecules and their interactions with light.<sup>96,103</sup> Further systematic research both experimental and theoretical is imperative for the fundamental understanding and potential applications of chiral NP chains and their promising applications including circular polarizers, detectors for circularly polarized light, asymmetric catalysts, and sensors of chiral biomolecules.

Overall, we believe that with continuing development in experimental methodology for the synthesis and self-assembly of metal NPs alongside the theoretical framework of description of the surface plasmon coupling based on the spatial configuration of the NP self-assemblies, research of nanoplasmonics will further expand, giving rise to novel effects, surprising discoveries and innovative applications in organic synthesis, sensing, solar cells, detection, etc.

#### Acknowledgements

H. X is grateful to Natural Science Foundation of China (51172126, 21473105 and 51002086) and Shandong Provincial

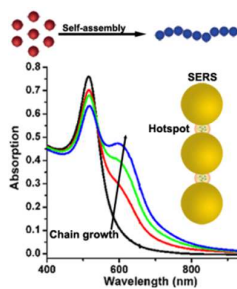
Science Fund for Distinguished Young Scholars (JQ201405) for the financial support. This work was also supported by program (NCET-10-0553). D. W. acknowledges the Australian Research Council for the financial support (DP 120102959).

## References

- S. A. Maier, *Plasmonics: Fundamentals and Applications*. Springer Verlag Press: New York, USA, 2007.
- K. L. Kelly, E. Coronado, L. L. Zhao and G. C. Schatz, *J. Phys. Chem. B*, 2003, **107**, 668-677.
- K. S. Lee and M. A. El-Sayed, *J. Phys. Chem. B*, 2006, **110**, 19220-19225.
- J. J. Mock, M. Barbic, D. R. Smith, D. A. Schultz and S. J. Schultz, *J. Chem. Phys.* 2002, **116**, 6755-6759.
- N. J. Halas, *MRS Bull.*, 2005, **30**, 362-367.
- S. K. Ghosh, S. Nath, S. Kundu, K. Esumi and T. Pal, *J. Phys. Chem. B*, 2004, **108**, 13963-13971.
- S. Underwood and P. Mulvaney, *Langmuir*, 1994, **10**, 3427-3430.
- M. M. Miller and A. A. Lazarides, *J. Phys. Chem. B*, 2005, **109**, 21556-21565.
- H. A. Atwater, *Scientific American*, 2007, **296**, 56-63.
- W. L. Barnes, A. Dereux and T.W. Ebbesen, *Nature*, 2003, **424**, 824-830.
- E. Ozbay, *Science*, 2006, **311**, 189-193.
- J. A. Schuller, E. S. Barnard, W. Cai, Y. C. Jun, J. S. White and M. L. Brongersma, *Nat. Mater.*, 2010, **9**, 193-204.
- C. F. Bohren and D. R. Huffman, *Absorption and Scattering of Light by Small Particles*, Wiley Interscience Press: New York, USA, 1983.
- H. Xia, S. Bai, J. Hartmann and D. Wang, *Langmuir*, 2010, **26**, 3585-3589.
- J. Rodríguez-Fernández, J. Pérez-Juste, F. Javier García de Abajo and L. M. Liz-Marzán, *Langmuir*, 2006, **22**, 7007-7010.
- H. Li, H. Xia, W. Ding, Y. Li, Q. Shi, D. Wang and X. Tao, *Langmuir*, 2014, **30**, 2498-2504.
- C. Novo, D. Gomez, J. Perez-Juste, Z. Y. Zhang, H. Petrova, M. Reisman, P. Mulvaney and G. V. Hartland, *Phys. Chem. Chem. Phys.*, 2006, **8**, 3540-3546.
- A. L. Schmucker, N. Harris, M. J. Banholzer, M. G. Blaber, K. D. Osberg, G. C. Schatz and C. A. Mirkin, *ACS Nano*, 2010, **4**, 5453-5463.
- V. Myroshnychenko, J. Rodriguez-Fernandez, I. Pastoriza-Santos, A. M. Funston, C. Novo, P. Mulvaney, L. M. Liz-Marzán and F. J. García de Abajo, *Chem. Soc. Rev.*, 2008, **37**, 1792-1805.
- R. Alvarez-Puebla, L. M. Liz-Marzán and F. J. García de Abajo, *J. Phys. Chem. Lett.*, 2010, **1**, 2428-2434.
- K. Su, Q. Wei, X. Zhang, J. J. Mock, D. R. Smith and S. Schultz, *Nano Lett.*, 2003, **3**, 1087-1090.
- E. Hao and G. C. Schatz, *J. Chem. Phys.*, 2004, **120**, 357-366.
- P. K. Jain, W. Huang and M. A. El-Sayed, *Nano Lett.*, 2007, **7**, 2080-2088.
- P. Bharadwaj, B. Deutsch and L. Novotny, *Adv. Opt. Photonics*, 2009, **1**, 438-483.
- J. Zuloaga, E. Prodan and P. Nordlander, *Nano Lett.*, 2009, **9**, 887-891.
- P. K. Jain, S. Eustis and M. A. El-Sayed, *J. Phys. Chem. B*, 2006, **110**, 18243.
- L. M. Liz-Marzán, T. Majima and D. G. Whitten, *Langmuir*, 2012, **28**, 8825-8825.
- M. Grzelczak and L. M. Liz-Marzán, *Langmuir*, 2013, **29**, 4652-4663.
- L. S. Slaughter, Y. Wu, B. A. Willingham, P. Nordlander and S. Link, *ACS Nano*, 2010, **4**, 4657-4666.
- J. Turkevich, P. C. Stevenson and J. A. Hillier, *Discuss. Faraday Soc.*, 1951, **11**, 55-75.
- Frens, G. *Nature (London): Phys. Sci.* 1973, **241**, 20-22.
- Ji, X.; Song, X.; Li, J.; Bai, Y.; Yang, W.; Peng, X. *J. Am. Chem. Soc.* 2007, **129**, 13939-13948.
- V. K. LaMer and R. H. Dinegar, *J. Am. Chem. Soc.*, 1950, **72**, 4847-4854.
- N. R. Jana, L. Gearheart and C. J. Murphy, *Langmuir*, 2001, **17**, 6782-6786.
- T. K. Sau and C. J. Murphy, *Langmuir*, 2004, **20**, 6414-6420.
- B. Nikoobakht and M. A. El-Sayed, *Chem. Mater.*, 2003, **15**, 1957-1962.
- C. Ziegler and A. Eychmüller, *J. Phys. Chem. C*, 2011, **115**, 4502-4506.
- N. G. Bastús, J. Comenge and V. Puntès, *Langmuir*, 2011, **27**, 11098-11105.
- X. Liu, H. Xu, H. Xia and D. Wang, *Langmuir*, 2012, **28**, 13720-13726.
- Z. Wang, B. Tan, I. Hussain, N. Schaeffer, M. F. Wyatt, M. Brust, and A. I. Cooper, *Langmuir*, 2007, **23**, 885-895.
- J. Kang, Y. Ding, B. Liu, and J. Yang, *Chem. Lett.*, 2015, **44**, 274-276.
- T. K. Sau and C. J. Murphy, *J. Am. Chem. Soc.*, 2004, **126**, 8648-8649.
- J. Zhang, M. R. Langille, M. L. Personick, K. Zhang, S. Li and C. A. Mirkin, *J. Am. Chem. Soc.*, 2010, **132**, 14012-14014.
- Y. Yu, Q. Zhang, X. Lu and J. Y. Lee, *J. Phys. Chem. C*, 2010, **114**, 11119-11126.
- X. Ye, Y. Gao, J. Chen, D. C. Reifsnyder, C. Zheng and C. B. Murray, *Nano Lett.*, 2013, **13**, 2163-2171.
- J. Zhang, C. Xi, C. Feng, H. Xia, D. Wang and X. Tao, *Langmuir*, 2014, **30**, 2480-2489.
- H. Xia, G. Su and D. Wang, *Angew. Chem. Int. Ed.*, 2013, **52**, 3726-3730.
- Z. Sun, W. Ni, Z. Yang, X. Kou, L. Li and J. Wang, *Small*, 2008, **4**, 1287-1292.
- Y. Liu, X. Han, L. He and Y. Yin, *Angew. Chem. Int. Ed.*, 2012, **51**, 6373-6377.
- H. Zhang, K. Fung, J. Hartmann, C. T. Chan and D. Wang, *J. Phys. Chem. C*, 2008, **112**, 16830-16839.
- M. A. Correa-Duarte, J. Pérez-Juste, A. Sánchez-Iglesias, M. Giersig and L. M. Liz-Marzán, *Angew. Chem. Int. Ed.*, 2005, **44**, 4375-4378.
- H. Wang, W. J. Lin, K. P. Fritz, G. D. Scholes, M. A. Winnik and I. Manners, *J. Am. Chem. Soc.*, 2007, **129**, 12924-12925.
- A. Sánchez-Iglesias, M. Grzelczak, J. Pérez-Juste and L. M. Liz-Marzán, *Angew. Chem. Int. Ed.*, 2010, **49**, 9985-9989.
- X. Shen, L. Chen, D. Li, L. Zhu, H. Wang, C. Liu, Y. Wang, Q. Xiong and H. Chen, *ACS Nano*, 2011, **5**, 8426-8433.
- A. P. Alivisatos, K. P. Johnsson, X. Peng, T. E. Wilson, C. J. Loweth, M. P. Bruchez and P. G. Schultz, *Nature*, 1996, **382**, 609-611.
- M. M. Maye, D. Nykypanchuk, M. Cuisinier, D. V der Lelie and O. Gang, *Nat. Mater.*, 2009, **8**, 388-391.
- M. M. Maye, M. T. Kumara, D. Nykypanchuk, W. B. Sherman and O. Gang, *Nat. Nanotechnol.*, 2010, **5**, 116-120.
- J. Sharma, R. Chhabra, A. Cheng, J. Brownell, Y. Liu, and H. Yan, *Science.*, 2009, **323**, 112-116.
- M. G. Warner, J. E. Hutchison, *Nat. Mater.*, 2003, **2**, 272-277.
- P. K. Lo, P. Karam, F.A. Aldaye, C. K. McLaughlin, G. D. Hamblin, G. Cosa and H. F. Sleiman, *Nat. Chem.*, 2010, **2**, 319-328.
- A. Kuzyk, R. Schreiber, Z. Fan, G. Pardatscher, E.-M. Roller, A. Högele, F. C. Simmel, A. O. Govorov and T. Liedl, *Nature*, 2012, **483**, 311-314.
- J. C. Love, L. A. Estroff, J. K. Kriebel, R. G. Nuzzo and G. M. Whitesides, *Chem. Rev.*, 2005, **105**, 1103-1170.

- 63 K. K. Caswell, J. N. Wilson, U. H. F. Bunz, and C. J. Murphy, *J. Am. Chem. Soc.*, 2003, **125**, 13914-13915.
- 64 S. Lin, M. Li, E. Dujardin, C. Girard and S. Mann, *Adv. Mater.*, 2005, **17**, 2553-2559.
- 65 A. Sancho, G. Baffou, R. Marty, A. Arbouet, R. Quidant, C. Girard and E. Dujardin, *ACS Nano*, 2012, **6**, 3434-3440.
- 66 A. Teulle, M. Bosman, C. Girard, K. L. Gurunatha, M. Li, S. Mann and E. Dujardin, *Nat. Mater.*, 2015, **14**, 87-94.
- 67 M. Sethi, G. Joung and M. R. Knecht, *Langmuir*, 2009, **25**, 1572-1581.
- 68 Z. Sun, W. Ni, Z. Yang, X. Kou, L. Li and J. Wang, *Small*, 2008, **4**, 1287-1292.
- 69 W. Ni, R. A. Mosquera, J. Pérez-Juste, L. M. Liz-Marzán, *J. Phys. Chem. Lett.*, 2010, **8**, 1181-1185.
- 70 H. Nakashima, K. Furukawa, Y. Kashimura and K. Torimitsu, *Chem. Commun.*, 2007, 1080-1082.
- 71 W. He, S. Hou, X. Mao, X. Wu, Y. Ji, J. Liu, X. Hu, K. Zhang, C. Wang, Y. Yang and Q. Wang, *Chem. Commun.*, 2011, **47**, 5482-5484.
- 72 D. A. Walker, C. E. Wilmer, B. Kowalczyk, K. J. Bishop and B. A. Grzybowski, *Nano Lett.*, 2010, **10**, 2275-2280.
- 73 N. Xiao and C. Yu, *Anal. Chem.*, 2010, **82**, 3659-3663.
- 74 C. V. Durgadas, V. N. Lakshmi, C. P. Sharma and K. Sreenivasan, *Sensor Actuat B-Chem*, 2011, **156**, 791-797.
- 75 H. Huang, X. Liu, T. Hu and P. K. Chu, *Biosens. Bioelectron.*, 2010, **25**, 2078-2083.
- 76 H. Zhang and D. Wang, *Angew. Chem. Int. Ed.* 2008, **47**, 3984-3987.
- 77 E. W. Edwards, M. Chanana, D. Wang, *J. Phys. Chem. C* 2008, **112**, 15207-15219.
- 78 Z. Nie, D. Fava, E. Kumacheva, S. Zou, G. Walker and M. Rubinstein, *Nat. Mater.*, 2007, **6**, 609-614.
- 79 K. Liu, A. Lukach, K. Sugikawa, S. Chung, J. Vickery, H. Thérien-Aubin, B. Yang, M. Rubinstein and E. Kumacheva, *Angew. Chem. Int. Ed.*, 2014, **126**, 2686-2691.
- 80 R. M. Choueiri, A. Klinkova, H. Thérien-Aubin, M. Rubinstein and E. Kumacheva, *J. Am. Chem. Soc.*, 2013, **135**, 10262-10265.
- 81 K. Liu, Z. Nie, N. Zhao, W. Li, M. Rubinstein and E. Kumacheva, *Science*, 2010, **329**, 197-200.
- 82 K. Liu, N. N. Zhao and E. Kumacheva, *Chem. Soc. Rev.*, 2011, **40**, 656-671.
- 83 S. Sheikholeslami, Y. Jun, P. K. Jain and A. P. Alivisatos, *Nano Lett.*, 2010, **10**, 2655-2660.
- 84 S. J. Barrow, A. M. Funston, D. E. Gómez, T. J. Davis and P. Mulvaney, *Nano Lett.*, 2011, **11**, 4180-4187.
- 85 S. J. Barrow, D. Rossouw, A. M. Funston, G. A. Botto and P. Mulvaney, *Nano Lett.*, 2014, **14**, 3799-3808.
- 86 A. Zabet-Khosousi and A.-A. Dhirani, *Chem. Rev.*, 2008, **108**, 4072-4124.
- 87 J. N. Anker, W. P. Hall, O. Lyandres, N. C. Shah, J. Zhao and R. P. Van Duyne, *Nat. Mater.*, 2008, **7**, 442-453.
- 88 L. Wang, Y. Zhu, L. Xu, W. Chen, H. Kuang, L. Liu, A. Agarwal, C. Xu and N. A. Kotov, *Angew. Chem., Int. Ed.*, 2010, **49**, 5472-5475.
- 89 A. Lee, G. F. S. Andrade, A. Ahmed, M. L. Souza, N. Coombs, E. Tumarkin, K. Liu, R. Gordon, A. G. Brolo and E. Kumacheva, *J. Am. Chem. Soc.*, 2011, **133**, 7563-7570.
- 90 G. Chen, Y. Wang, M. Yang, J. Xu, S. J. Goh, M. Pan and H. Chen, *J. Am. Chem. Soc.*, 2010, **132**, 3644-3645.
- 91 D. K. Lim, K. S. Jeon, H. M. Kim, J. M. Nam and Y. D. Suh, *Nat. Mater.*, 2010, **9**, 60-67.
- 92 T. Chen, H. Wang, G. Chen, Y. Wang, Y. H. Feng, W. S. Teo, T. Wu and H. Chen, *ACS Nano*, 2010, **4**, 3087-3094.
- 93 Y. Xia, Y. L. Zhou and Z. Y. Tang, *Nanoscale*, 2011, **3**, 1374-1382.
- 94 Z. Zhu, W. Liu, Z. Li, B. Han, Y. Zhou, Y. Gao and Z. Tang, *ACS Nano*, 2012, **6**, 2326-2332.
- 95 W. Chen, A. Bian, A. Agarwal, L. Liu, H. Shen, L. Wang, C. Xu and N. A. Kotov, *Nano Lett.*, 2009, **9**, 2153-2159.
- 96 X. Wu, L. Xu, L. Liu, W. Ma, H. Yin, H. Kuang, L. Wang, C. Xu and N. A. Kotov, *J. Am. Chem. Soc.*, 2013, **135**, 18629-18636.
- 97 A. Guerrero-Martínez, M. Grzelczak and L. M. Liz-Marzán, *ACS Nano*, 2012, **6**, 3655-3662.
- 98 L. S. Slaughter, B. A. Willingham, W. S. Chang, M. H. Chester, N. Ogden and S. Link, *Nano Lett.*, 2012, **12**, 3967-3972.
- 99 K. Liu, A. Ahmed, S. Chung, K. Sugikawa, G. Wu, Z. Nie, R. Gordon and E. Kumacheva, *ACS Nano*, 2013, **7**, 5901-5910.
- 100 M. Rycenga, C. M. Cobley, J. Zeng, W. Li, C. H. Moran, Q. Zhang, D. Qin and Y. N. Xia, *Chem. Rev.*, 2011, **111**, 3669-3712.
- 101 H. Li, H. Xia, D. Wang and X. Tao, *Langmuir*, 2013, **29**, 5074-5079.
- 102 H. Li, H. Xia, W. Ding, Y. Li, Q. Shi, D. Wang and X. Tao, *Langmuir*, 2014, **30**, 2498-2504.
- 103 V. K. Valev, J. J. Baumberg, C. Sibilia and T. Verbiest, *Adv. Mater.*, 2013, **25**, 2517-2534.

## Graphic Abstract



The review is an overview of the current developments in directed self-assembly of metal nanoparticles with tailored plasmonic properties.